

A.V.Kotikov, JINR, Dubna

(in collab. with I.R. Gabdrakhmanov, N.A Gramotkov, O.V. Teryaev, D.A. Volkova
and I.A. Zemlyakov, JINR, Dubna).

based on JETP Lett. 118 (2023) 7, 478-482 [2307.16225 [hep-ph]]
and 2404.01873 [hep-ph]

**Efim Fradkin Centennial Conference Moscow, Russia, September
2–6, 2024**

**Bjorken sum rule with analytic coupling. Heavy
quark contributions.**

OUTLINE

1. Introduction
2. Results
3. Conclusions

Abstract

The experimental data obtained for the polarized Bjorken sum rule $\Gamma_1^{p-n}(Q^2)$ for small values of Q^2 are approximated by the predictions obtained in the framework of analytic QCD up to the 5th order perturbation theory, whose coupling constant does not contain the Landau pole. We found an excellent agreement between the experimental data and the predictions of analytic QCD, as well as a strong difference between these data and the results obtained in the framework of standard QCD. To satisfy the limit of photoproduction and take into account Gerasimov-Drell-Hearn and Burkhardt-Cottingham sum rules, we developed new representation of the perturbative part of the polarized Bjorken sum rule.

0. Introduction

Polarized Bjorken sum rule (BSR) $\Gamma_1^{p-n}(Q^2)$ (Bjorken: 1966), i.e. the difference between the first moments of the spin-dependent structure functions (SFs) of a proton and neutron, is a very important space-like QCD observable (Deur, Brodsky, De Téramond: 2018), (Kuhn, Chen, Leader: 2009).

Its isovector nature facilitates its theoretical description in perturbative QCD (pQCD) in terms of the operator product expansion (OPE), compared to the corresponding SF integrals for each nucleon.

Experimental results for this quantity obtained in polarized deep inelastic scattering (DIS) are currently available in a wide range of the spacelike squared momenta Q^2 : $0.021 \text{ GeV}^2 \leq Q^2 < 5 \text{ GeV}^2$ (see, e.g., (Deur et al.: 2022) and references therein).

Theoretically, pQCD (with OPE) in the \overline{MS} -scheme was the usual approach to describing such quantities. This approach, however, has the theoretical disadvantage that the running coupling constant (*couplant*) $\alpha_s(Q^2)$ has the Landau singularities for small Q^2 values: $Q^2 \leq 0.1 \text{ GeV}^2$, which makes it inconvenient for estimating spacelike observables at small Q^2 , such as BSR.

In the recent years, the extension of pQCD couplings for low Q^2 without Landau singularities called (fractional) analytic perturbation theory [(F)APT)] (Shirkov, Solovtsov: 1996,1997), (Milton, Solovtsov, Solovtsova: 1997), (Shirkov: 2001) and (Bakulev, Mikhailov, Stefanis: 2007,2007,2010) (or the minimal analytic (MA) theory (Cvetic, Valenzuela: 2008,2011)), were applied to match the theoretical OPE expression with the experimental BSR data (Pasechnik et al.: 2008,2010,2012), (Ayala et al.: 2017,2018).

0+. History. QED.

Consider so-called polarization operator $D(k^2)$ in QED. Leading logarithmic terms of $D(k^2)$ in the n order of perturbation theory with $|k^2| \gg m^2$ (m is the electron mass) have the following form:

$$(e^2 F(K^2, m^2))^n / K^2, \quad K^2 = -k^2 \geq 0, \quad F(K^2, m^2) = \frac{1}{3\pi} \ln \left(\frac{K^2}{4m^2} \right).$$

Resummation of the large logarithms leads to
(Landau, Abrikosov, Khalatnikov:1954):

$$D_{\text{per}}(k^2) = \frac{1}{K^2} \frac{1}{1 - \frac{e^2}{3\pi} \ln \left(\frac{K^2}{4m^2} \right)}.$$

Then, there is the pole (so-called Landau pole) at K_p^2 :

$$K_p^2 = 4m^2 e^{3\pi/e^2}$$

and QED is not applicable at $K^2 \geq K_p^2$ (Landau, Pomeranchuk:1955).

With another side, there is so-called Kallen-Lehmann representation:

$$D(k^2) = \frac{1}{K^2} + \int_{4m^2}^{\infty} dz \frac{I(z)}{z + K^2}, \quad I(z) = \text{Im}D(i\varepsilon - K^2)$$

and $D_{\text{per}}(k^2)$ is not in agreement with the Kallen-Lehmann representation.

Combination of the Kallen-Lehmann representation and perturbation theory (*or same, perturbation theory for $I(z)$*) has been considered in (Redmond:1958), (Redmond,Uretsky:1958), (Bogolyubov,Logunov,Shirkov:1959).

We follow (Bogolyubov, Logunov, Shirkov:1959).

From calculation (Landau, Abrikosov, Khalatnikov:1954) they obtained that $I_{\text{per}}(z) = 0$ for $z < 4m^2$ and for $z \geq 4m^2$:

$$I_{\text{per}}(z) = \frac{e^2}{3\pi z} \frac{1}{\left(1 - \frac{e^2}{3\pi} \ln\left(\frac{z-4m^2}{4m^2}\right)\right)^2 + \frac{e^2}{9}}.$$

Using $I_{\text{per}}(z)$ in the Kallen-Lehmann representation they obtained at $|k^2| \gg m^2$

$$D(k^2) = \frac{1}{K^2} \frac{1}{1 - \frac{e^2}{3\pi} \ln\left(\frac{K^2}{4m^2}\right)} + \frac{(3\pi)/e^2}{K^2 - K_p^2}.$$

The additional term cancels exactly Landau pole at $K^2 = K_p^2$. Moreover, it cannot be obtained in the framework of perturbation theory, since it cannot be expanded in e^2 -series.

Thus, the combination of perturbation theory and Kallen-Lehmann representation (i.e. perturbation theory for spectral function) does not lead to the Landau problem in QED.

In the general case the QCD couplant is defined as a product of propagators and a vertex function. Therefore, one might pose a question concerning the analytic properties of this quantity. This matter has been examined ([Ginzburg,Shirkov:1965](#)).

It was shown that in this case the integral representation of the Kallen-Lehmann type holds for the running coupling, too. Proceeding from these motivations, the analytic approach was lately extended to Quantum Chromodynamics by D.V. Shirkov and I.L. Solovtsov.

1. Analytic coupling constant

According to the general principles of (local) quantum field theory (QFT) (Bogolyubov, Shirkov:1959); (Oehme:1994) observables in the spacelike domain can have singularities only with negative values of their argument Q^2 .

On the other hand, for large values of Q^2 , these observables are usually represented as power series expansion by the running coupling constant (couplant) $\alpha_s(Q^2)$, which, in turn, has a ghost singularity, the so-called Landau pole, for $Q^2 = \Lambda^2$.

To restore analyticity, this pole must be removed.

Strong couplant $\alpha_s(Q^2)$ obeys the renormalized group equation

$$L \equiv \ln \frac{Q^2}{\Lambda^2} = \int \bar{a}_s(Q^2) \frac{da}{\beta(a)}, \quad \bar{a}_s(Q^2) = \frac{\alpha_s(Q^2)}{4\pi}, \quad a_s(Q^2) = \beta_0 \bar{a}_s(Q^2)$$

with some boundary condition and the QCD β -function:

$$\beta(a_s) = - \sum_{i=0} \beta_i \bar{a}_s^{i+2} = -\beta_0 \bar{a}_s^2 (1 + \sum_{i=1} b_i \bar{a}_s^i), \quad b_i = \frac{\beta_i}{\beta_0^{i+1}},$$

where the first fifth coefficients, i.e. β_i with $i \leq 4$, are exactly known ([Baikov, Chetyrkin, Kuhn: 2017](#)).

So, already at leading order (LO), when $a_s(Q^2) = a_s^{(1)}(Q^2)$, we have

$$a_s^{(1)}(Q^2) = \frac{1}{L},$$

i.e. $a_s^{(1)}(Q^2)$ does contain a pole at $Q^2 = \Lambda^2$.

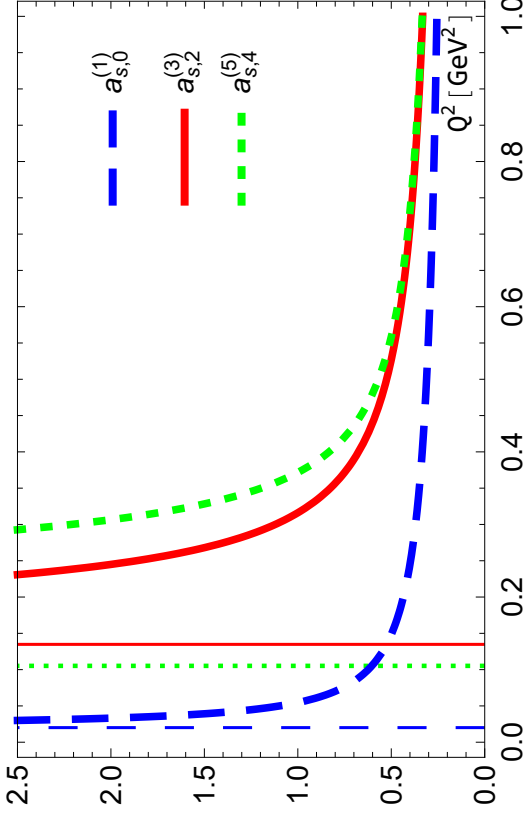


Figure 1: The results for $a_{s,i}^{(i+1)}(Q^2)$ and $(\Lambda_i^{f=3})^2$ (vertical lines) with $i = 0, 2, 4$.

In Fig. 1 one can see that the strong couplants $a_{s,i}^{(i+1)}(Q^2)$ become to be singular at $Q^2 = \Lambda_i^2$. The Λ_0 and Λ_i ($i \geq 1$) values are rather different (Chen,Liu,Wang,Waqas,Peng: 2021):

$$\Lambda_0^{f=3} = 142 \text{ MeV}, \quad \Lambda_1^{f=3} = 367 \text{ MeV}, \quad \Lambda_2^{f=3} = 324 \text{ MeV},$$

$$\Lambda_3^{f=3} = 328 \text{ MeV}.$$

In a series of papers (Shirkov,Solovtsov: 1996,1997); (Milton,Solovtsov,Solovtsova: 1997); (Shirkov: 2001) authors have developed an effective approach to eliminate the Landau singularity without introducing extraneous IR regulators.

The idea: the dispersion relation, which connects the new analytic couplant $A_{\text{MA}}(Q^2)$ with the spectral function $r_{\text{pt}}(s)$, obtained in the framework of perturbative theory. In LO

$$A_{\text{MA}}^{(1)}(Q^2) = \frac{1}{\pi} \int_0^{+\infty} \frac{ds}{(s+t)} r_{\text{pt}}^{(1)}(s), \quad r_{\text{pt}}^{(1)}(s) = \text{Im } a_s^{(1)}(-s - i\epsilon),$$

So, let's repeat once again: the spectral function is taken directly from perturbation theory, but the analytic couplant $A_{MA}(Q^2)$ is restored using dispersion relations.

This approach is called *Minimal Approach (MA)* (Cvetic, Valenzuela: 2008) or *Analytic Perturbation Theory (APT)* (Shirkov, Solovtsov:1996,1997); (Milton,Solovtsov,Solovtsova:1997); (Shirkov:2001)

Thus, MA QCD is a very convenient approach that combines the general (analytical) properties of quantum field quantities and the results obtained within the framework of perturbative QCD, leading to the appearance of the MA couplant $A_{MA}(Q^2)$, which is close to the usual strong couplant $a_s(Q^2)$ in the limit of large values of its argument and completely different at $Q^2 \leq \Lambda^2$.

A further development of APT is the so-called fractional APT (FAPT), which extends the principles of constructing to non-integer powers of couplant, which arise for many quantities having non-zero anomalous dimensions ([Bakulev, Mikhailov, Stefanis: 2005, 2008, 2010](#)), with some previous study ([Karanikas, Stefanis: 2001](#)) and reviews ([Bakulev: 2008](#)), ([Stefanis: 2013](#)).

The results in FATP have a very simple form in LO perturbation theory, but they are quite complicated in higher orders.

1.1 LO

The LO minimal analytic coupling $A_{\text{MA},\nu}^{(1)}$ have the form
(Bakulev, Mikhailov, Stefanis: 2005)

$$A_{\text{MA},\nu,0}^{(1)}(Q^2) = \left(a_{\nu,0}^{(1)}(Q^2) \right)^\nu - \frac{\text{Li}_{1-\nu}(z_0)}{\Gamma(\nu)} \equiv \frac{1}{L_0^\nu} - \Delta_{\nu,0}^{(1)},$$

where

$$\text{Li}_\nu(z) = \sum_{m=1}^{\infty} \frac{z^m}{m^\nu} = \frac{z}{\Gamma(\nu)} \int_0^\infty \frac{dt t^{\nu-1}}{(et-z)}, \quad z_i = \frac{\Lambda_i^2}{Q^2}$$

is the Polylogarithmic function.

For $\nu = 1$ we recover the famous Shirkov-Solovtsov result (Shirkov, Solovtsov: 1996)

$$A_{\text{MA},0}^{(1)}(Q^2) \equiv A_{\text{MA},\nu=1,0}^{(1)}(Q^2) = a_{s,0}^{(1)}(Q^2) - \frac{z_0}{1-z_0} = \frac{1}{L_0} - \frac{z_0}{1-z_0}.$$

1.2 Beyond LO

Following (Cvetic, Valenzuela: 2006), we introduce here the derivatives (in the k -order of perturbation theory (PT))

$$\tilde{a}_{n+1}^{(k)}(Q^2) = \frac{(-1)^n d^n a_s^{(k)}(Q^2)}{n! (dL)^n}, a_s^{(k)}(Q^2) = \frac{\beta_0 \alpha_s^{(k)}(Q^2)}{4\pi} = \beta_0 \bar{a}_s^{(k)}(Q^2),$$

which are very convenient in the case of analytic QCD. β_0 is the first coefficient of the QCD β -function:

$$\beta(\bar{a}_s^{(k)}) = -(\bar{a}_s^{(k)})^2 \left(\beta_0 + \sum_{i=1}^k \beta_i (\bar{a}_s^{(k)})^i \right),$$

where β_i are known up to $k = 4$ (Baikov, Chetyrkin, Kuhn: 2008).

The series of derivatives $\tilde{a}_n(Q^2)$ can successfully replace the corresponding series of a_s -powers (see, e.g. [\(Kotikov, Zemlyakov: 2022\)](#)). Indeed, each derivative reduces the a_s power but is accompanied by an additional β -function $\sim a_s^2$. Thus, each application of a derivative yields an additional a_s , and thus it is indeed possible to use a series of derivatives instead of a series of a_s -powers.

In LO, the series of derivatives $\tilde{a}_n(Q^2)$ are exactly the same as a_s^n . Beyond LO, the relationship between $\tilde{a}_n(Q^2)$ and a_s^n was established in [\(Cvetic, Valenzuela: 2006\)](#), [\(Cvetic, Kogerler, Valenzuela: 2010\)](#) and extended to the fractional case, where $n \rightarrow$ is a non-integer ν , in [\(Cvetic, Kotikov: 2012\)](#)

Now we consider the $1/L$ expansion of $\tilde{a}_\nu^{(k)}(Q^2)$. After some calculations, we have

$$\begin{aligned}\tilde{a}_{\nu,0}^{(1)}(Q^2) &= (a_{s,0}^{(1)}(Q^2))^\nu = \frac{1}{L_0^\nu}, \\ \tilde{a}_{\nu,i}^{(i+1)}(Q^2) &= \tilde{a}_{\nu,i}^{(1)}(Q^2) + \sum_{m=1}^i C_m^{\nu+m} \tilde{\delta}_{\nu,i}^{(m+1)}(Q^2), \\ \tilde{\delta}_{\nu,i}^{(m+1)}(Q^2) &= \hat{R}_m \frac{1}{L_i^{\nu+m}}, \quad C_m^{\nu+m} = \frac{\Gamma(\nu+m)}{m!\Gamma(\nu)},\end{aligned}$$

where

$$\hat{R}_1 = b_1 \left[\hat{Z}_1(\nu) + \frac{d}{d\nu} \right], \quad \hat{R}_2 = b_2 + b_1^2 \left[\frac{d^2}{(d\nu)^2} + 2\hat{Z}_1(\nu+1) \frac{d}{d\nu} + \hat{Z}_2(\nu+1) \right].$$

The representation of the $\tilde{\delta}_{\nu,i}^{(m+1)}(Q^2)$ corrections as \hat{R}_m -operators is very important to use. This will make it possible to present high-order results for the analytic couplant in a similar way.

Here

$$Z_2(\nu) = S_1^2(\nu) - S_2(\nu),$$

$$Z_1(\nu) \equiv S_1(\nu) = \Psi(1 + \nu) + \gamma_E, \quad S_2(\nu) = \zeta_2 - \Psi'(1 + \nu),$$

and

$$S_m(N) = \sum_{k=1}^N \frac{1}{k^m}, \quad \hat{Z}_1(\nu) = Z_1(\nu) - 1, \quad \hat{Z}_2(\nu) = Z_2(\nu) - 2Z_1(\nu) + 1.$$

Note that operators like $(d/d\nu)^m$ were used earlier in (Bakulev, Mikhailov, Stefanishin, 2005, 2008, 2010).

Here we apply the inverse logarithmic expansion of the MA couplings, recently obtained in (Kotikov, Zemlyakov: 2023) for any PT order. This approach is very convenient: for LO the MA couplings have simple representations (see (Bakulev, Mikhailov, Stefanis: 2007,2007,2010)), while beyond LO the MA couplings are very close to LO ones, especially for $Q^2 \rightarrow \infty$ and $Q^2 \rightarrow 0$, where the differences between MA couplings of various PT orders become insignificant. Moreover, for $Q^2 \rightarrow \infty$ and $Q^2 \rightarrow 0$ the (fractional) derivatives of the MA couplings with $n \geq 2$ tend to zero, and therefore only the first term in perturbative expansions makes a valuable contribution.

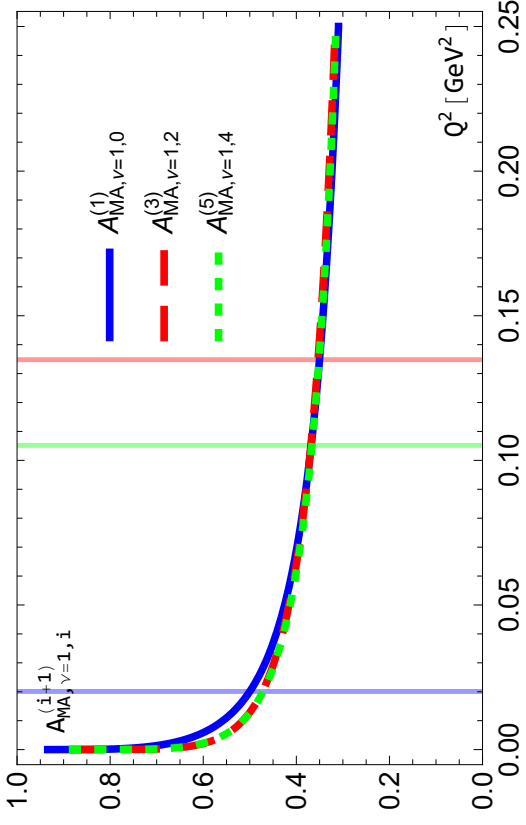


Figure 2: The results for $A_{\text{MA}, \nu=1, i}^{(i+1)}(Q^2)$ with $i = 0, 2, 4$.

From Fig. 2 we can see differences between $A_{\text{MA}, \nu=1, i}^{(i+1)}(Q^2)$ with $i = 0, 2, 4$, which are rather small and have nonzero values around the position $Q^2 = \Lambda_i^2$.

2. Bjorken sum rule

The polarized (nonsinglet) BSR is defined as the difference between the proton and neutron polarized SFs, integrated over the entire interval x

$$\Gamma_1^{p-n}(Q^2) = \int_0^1 dx [g_1^p(x, Q^2) - g_1^n(x, Q^2)].$$

Theoretically, the quantity can be written in the OPE form (Shuryak, Vainshtein: 1982), (Balitsky, Braun, Kolesnichenko: 1990)

$$\Gamma_1^{p-n}(Q^2) = \frac{g_A}{6} (1 - D_{BS}(Q^2)) + \sum_{i=2}^{\infty} \frac{\mu_{2i}(Q^2)}{Q^{2i-2}},$$

where $g_A=1.2762 \pm 0.0005$ (PDG: 2020) is the nucleon axial charge, $(1 - D_{BS}(Q^2))$ is the leading-twist contribution, and μ_{2i}/Q^{2i-2} ($i \geq 1$) are the higher-twist (HT) contributions.

Since we include very small Q^2 values here, this representation of the HT contributions is inconvenient. It is much better to use the so-called “massive” representation for the HT part (introduced in (Teryaev: 2013), (Khandramai, Teryaev, Gabdrakhmanov: 2016)):

$$\Gamma_1^{p-n}(Q^2) = \frac{g_A}{6} (1 - D_{\text{BS}}(Q^2)) + \frac{\hat{\mu}_4 M^2}{Q^2 + M^2},$$

where the values of $\hat{\mu}_4$ and M^2 have been fitted in (Ayala et al.: 2018) in the different analytic QCD models.

In the case of MA QCD, from (Ayala et al.: 2018)

$$M^2 = 0.439 \pm 0.012 \pm 0.463, \quad \hat{\mu}_{\text{MA},4} = -0.173 \pm 0.002 \pm 0.666,$$

where the statistical (small) and systematic (large) uncertainties are presented.

Up to the k -th PT order, the perturbative part has the form

$$D_{\text{BS}}^{(1)}(Q^2) = \frac{4}{\beta_0} a_s^{(1)}, D_{\text{BS}}^{(k \geq 2)}(Q^2) = \frac{4}{\beta_0} a_s^{(k)} \left(1 + \sum_{m=1}^{k-1} d_m (a_s^{(k)})^m \right),$$

where d_1 , d_2 and d_3 are known from exact calculations. The exact d_4 value is not known, but it was recently estimated in (Ayala, Pineda: 2022))

Converting the powers of couplant into its derivatives, we have

$$D_{\text{BS}}^{(1)}(Q^2) = \frac{4}{\beta_0} \tilde{a}_1^{(1)}, D_{\text{BS}}^{(k \geq 2)}(Q^2) = \frac{4}{\beta_0} \left(\tilde{a}_1^{(k)} + \sum_{m=2}^k \tilde{d}_{m-1} \tilde{a}_m^{(k)} \right),$$

where $b_i = \beta_i / \beta_0^{i+1}$ and

$$\begin{aligned} \tilde{d}_1 &= d_1, & \tilde{d}_2 &= d_2 - b_1 d_1, & \tilde{d}_3 &= d_3 - \frac{5}{2} b_1 d_2 - \left(b_2 - \frac{5}{2} b_1^2 \right) d_1, \\ \tilde{d}_4 &= d_4 - \frac{13}{3} b_1 d_3 - \left(3b_2 - \frac{28}{3} b_1^2 \right) d_2 - \left(b_3 - \frac{22}{3} b_1 b_2 + \frac{28}{3} b_1^3 \right) d_1. \end{aligned}$$

For the case of 3 active quark flavors ($f = 3$), we have

$$\begin{aligned} d_1 &= 1.59, & d_2 &= 3.99, & d_3 &= 15.42 & d_4 &= 63.76, \\ \tilde{d}_1 &= 1.59, & \tilde{d}_2 &= 2.73, & \tilde{d}_3 &= 8.61, & \tilde{d}_4 &= 21.52, \end{aligned}$$

i.e., the coefficients in the series of derivatives are slightly smaller.

In MA QCD, the results for BSR become as follows

$$\Gamma_{\text{MA},1}^{p-n}(Q^2) = \frac{g_A}{6} (1 - D_{\text{MA,BS}}(Q^2)) + \frac{\hat{\mu}_{\text{MA},4} M^2}{Q^2 + M^2},$$

where the perturbative part $D_{\text{BS,MA}}(Q^2)$ takes the form

$$D_{\text{MA,BS}}^{(1)}(Q^2) = \frac{4}{\beta_0} A_{\text{MA}}^{(1)},$$

$$D_{\text{MA,BS}}^{k \geq 2}(Q^2) = \frac{4}{\beta_0} (A_{\text{MA}}^{(k)} + \sum_{m=2}^k \tilde{d}_{m-1} \tilde{A}_{\text{MA},\nu=m}^{(k)}).$$

	M^2 for $Q^2 \leq 5 \text{ GeV}^2$ (for $Q^2 \leq 0.6 \text{ GeV}^2$)	$\hat{\mu}_{\text{MA},4}$ for $Q^2 \leq 5 \text{ GeV}^2$ (for $Q^2 \leq 0.6 \text{ GeV}^2$)	$\chi^2/(\text{d.o.f.})$ for $Q^2 \leq 5 \text{ GeV}^2$ (for $Q^2 \leq 0.6 \text{ GeV}^2$)
LO	0.472 ± 0.035 (1.631 ± 0.301)	-0.212 ± 0.006 (-0.166 ± 0.001)	0.667 (0.789)
NLO	0.414 ± 0.035 (1.545 ± 0.287)	-0.206 ± 0.008 (-0.155 ± 0.001)	0.728 (0.757)
N ² LO	0.397 ± 0.034 (1.417 ± 0.241)	-0.208 ± 0.008 (-0.156 ± 0.002)	0.746 (0.728)
N ³ LO	0.394 ± 0.034 (1.429 ± 0.248)	-0.209 ± 0.008 (-0.157 ± 0.002)	0.754 (0.747)
N ⁴ LO	0.397 ± 0.035 (1.462 ± 0.259)	-0.208 ± 0.007 (-0.157 ± 0.001)	0.753 (0.754)

Table 1: The values of the fit parameters.

3. Results

The fitting results of experimental data obtained only with statistical uncertainties are presented in Table 3 and shown in Figs. 3 and 4. For the fits we use Q^2 -independent M^2 and $\hat{\mu}_4$ and the two-twist parts for regular PT and APT, respectively.

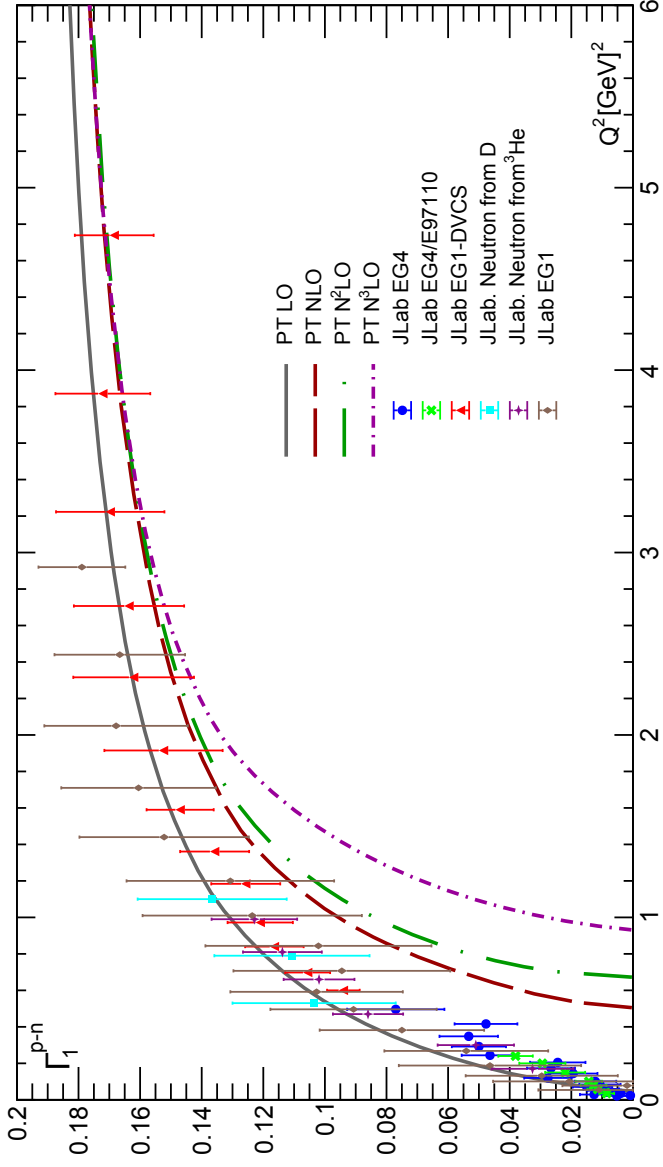


Figure 3: The results for $\Gamma_1^{p-n}(Q^2)$ in the first four orders of PT.

As it can be seen in Fig. 3, with the exception of LO, the results obtained using conventional couplant are very poor. Moreover, the discrepancy in this case increases with the order of PT.

The LO results describe experimental points relatively well, since the value of Λ_{LO} is quite small compared to other Λ_i , and disagreement with the data begins at lower values of Q^2 (see Fig. 4 below).

Thus, using the “massive” twist-four form does not improve these results, since with $Q^2 \rightarrow \Lambda_i^2$ conventional couplants become singular, which leads to large and negative results for the twist-two part (see above). So, as the PT order increases, ordinary couplants become singular for ever larger Q^2 values, while BSR tends to negative values for ever larger Q^2 values.

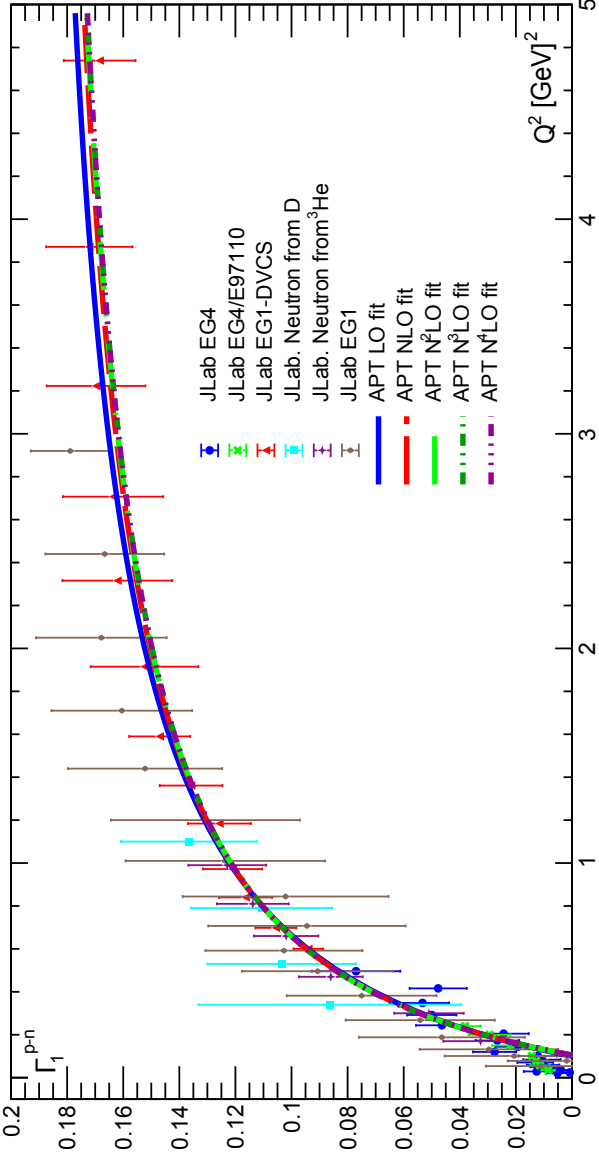


Figure 4: The results for $\Gamma_1^{p-n}(Q^2)$ in the first four orders of APT.

In contrast, our results obtained for different APT orders are practically equivalent: the corresponding curves become indistinguishable when Q^2 approaches 0 and slightly different everywhere else. As can be seen in Fig. 4, the fit quality is pretty high, which is demonstrated by the values of the corresponding $\chi^2/(d.o.f.)$ (see Table 3).

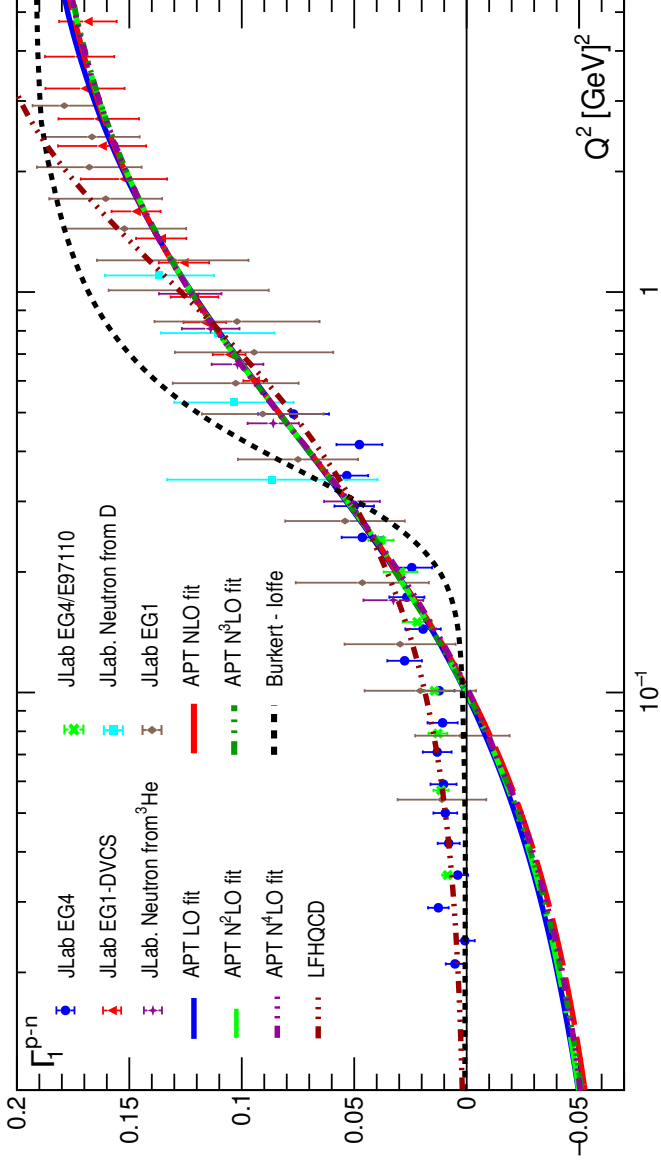


Figure 5: Same as in Fig. 4 but for $Q^2 < 0.6 \text{ GeV}^2$.

3.1 Low Q^2 values

The full picture, however, is more complex than shown in Fig. 4. The APT fitting curves become negative (see Fig. 10) when we move to very low values of Q^2 : $Q^2 < 0.1 \text{ GeV}^2$.

So, the good quality of the fits shown in Table 3 was obtained due to good agreement with experimental data at $Q^2 > 0.2 \text{ GeV}^2$. The picture improves significantly when we compare our result with experimental data for $Q^2 < 0.6 \text{ GeV}^2$ (see Fig. 6).

Fig. 6 also shows contributions from conventional PT in the first two orders: the LO and NLO predictions have nothing in common with experimental data. As we mentioned above, higher orders lead to even worse agreement, and they are not shown.

The purple curve emphasizes the key role of the twist-four contribution. Excluding this contribution, the value of $\Gamma_1^{p-n}(Q^2)$ is about 0.16, which is very far from the experimental data.

At $Q^2 \leq 0.3 \text{ GeV}^2$, we also see the good agreement with the phenomenological models.

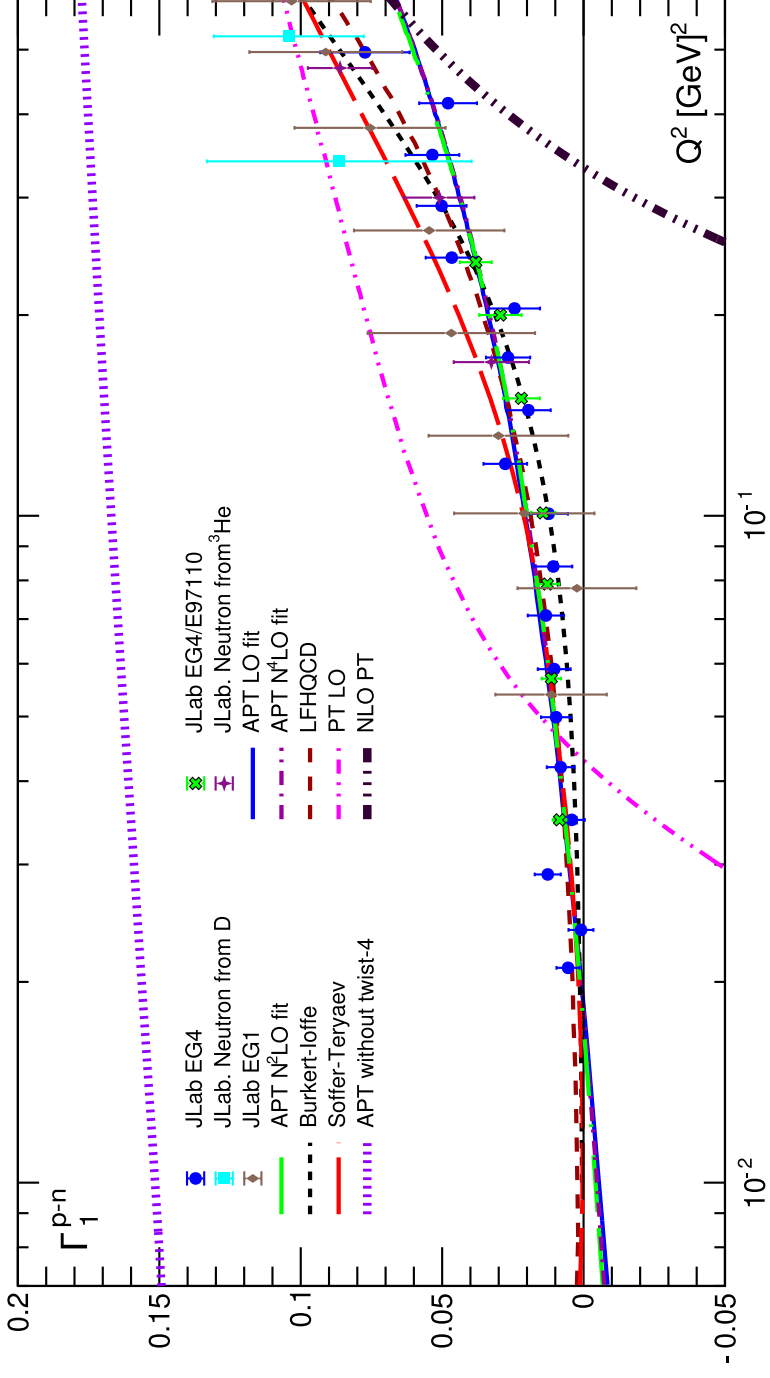


Figure 6: The results for $\Gamma_1^{p-n}(Q^2)$ in the first four orders of APT from fits of experimental data with $Q^2 < 0.6 \text{ GeV}^2$

For larger values of Q^2 , our results are lower than the results of phenomenological models, and for $Q^2 \geq 0.5 \text{ GeV}^2$ below the experimental data.

Nevertheless, even in this case where very good agreement with experimental data with $Q^2 < 0.6 \text{ GeV}^2$ is demonstrated, our results for $\Gamma_{\text{MA},1}^{p-n}(Q^2)$ take negative unphysical values when $Q^2 < 0.02 \text{ GeV}^2$. The reason for this phenomenon can be shown by considering photoproduction within APT.

3.2 Photoproduction

To understand the problem $\Gamma_{\text{MA},1}^{p-n}(Q^2 \rightarrow 0) < 0$, we consider the photoproduction case. In the k -th order of MA QCD

$$A_{\text{MA}}^{(k)}(Q^2 = 0) \equiv \tilde{A}_{\text{MA},m=1}^{(k)}(Q^2 = 0) = 1, \quad \tilde{A}_{\text{MA},m}^{(k)} = 0, \quad \text{when } m > 1$$

and, so, we have

$$D_{\text{MA,BS}}(Q^2 = 0) = \frac{4}{\beta_0} \quad \text{and, hence,}$$

$$\Gamma_{\text{MA},1}^{p-n}(Q^2 = 0) = \frac{g_A}{6} \left(1 - \frac{4}{\beta_0}\right) + \hat{\mu}_{\text{MA},4}.$$

The finiteness of cross-section in the real photon limit leads to

$$\Gamma_{\text{MA},1}^{p-n}(Q^2 = 0) = 0 \text{ and, thus, } \hat{\mu}_{\text{MA},4}^{php} = -\frac{g_A}{6} \left(1 - \frac{4}{\beta_0}\right).$$

For $f = 3$, we have

$$\hat{\mu}_{\text{MA},4}^{php} = -0.118 \text{ and, hence, } |\hat{\mu}_{\text{MA},4}^{php}| < |\hat{\mu}_{\text{MA},4}|,$$

shown in Table 3.

So, the finiteness of the cross section in the real photon limit is violated in our approaches.

This violation leads to negative values of $\Gamma_{\text{MA},1}^{p-n}(Q^2 \rightarrow 0)$.

Note that the results for $\hat{\mu}_{\text{MA},4}$ were obtained taking into account only statistical uncertainties. When adding systematic uncertainties, the results for $\hat{\mu}_{\text{MA},4}^{php}$ and $\hat{\mu}_{\text{MA},4}$ are completely consistent with each other, but the predictive power of such an analysis is small.

This violation is less for experimental data sets with $Q^2 \leq 0.6 \text{GeV}^2$, where the obtained values for $|\hat{\mu}_{\text{MA},4}|$ are essentially less than those obtained in the case of experimental data with $Q^2 \leq 5 \text{GeV}^2$. Smaller values of $|\hat{\mu}_{\text{MA},4}|$ lead to negative values of $\Gamma_{\text{MA},1}^{p-n}(Q^2 \rightarrow 0)$, when $Q^2 \leq 0.02 \text{GeV}^2$ (see Fig. 4).

3.3 Gerasimov-Drell-Hearn and Burkhardt-Cottingham sum rules

Now we plan to improve our analysis by taking into account the “massive” twist-six term.

Moreover, we take into account also the Gerasimov-Drell-Hearn and Burkhardt-Cottingham sum rules

$$\frac{d}{dQ^2} \Gamma_{MA,1}^{p-n}(Q^2 = 0) = G, \quad G = \frac{\mu_n^2 - (\mu_p - 1)^2}{8M_p^2} = 0.0631,$$

where $\mu_n = -1.91$ and $\mu_p = 2.79$ are proton and neutron magnetic moments, respectively, and $M_p = 0.938$ GeV is a nucleon mass. Note that the value of G is small.

In agreement with the definition, we have that

$$Q^2 \frac{d}{dQ^2} \tilde{A}_n(Q^2) \sim \tilde{A}_{n+1}(Q^2).$$

Then, for $Q^2 \rightarrow 0$ we obtain at any n value, that

$$Q^2 \frac{d}{dQ^2} \tilde{A}_n(Q^2) \rightarrow 0,$$

but very slowly, that the derivative

$$\frac{d}{dQ^2} \tilde{A}_n(Q^2 \rightarrow 0) \rightarrow \infty.$$

Thus, after application the derivative d/dQ^2 for $\Gamma_{\text{MA},1}^{p-n}(Q^2)$, **every term in $D_{\text{MA,Bs}}(Q^2)$** becomes to be divergent at $Q^2 \rightarrow 0$.

To produce finiteness at $Q^2 \rightarrow 0$ for the l.h.s. of $\Gamma_{\text{MA},1}^{p-n}(Q^2 \rightarrow 0)$, we can assume the relation between twist-two and twist-four terms, that leads to the appearance of a new contribution

$$-\frac{g_A}{6} D_{\text{MA,BS}}(Q^2) + \frac{\hat{\mu}_{\text{MA},4} M^2}{Q^2 + M^2} D_{\text{MA,BS}}(Q^2),$$

which can be done to be regular at $Q^2 \rightarrow 0$.

This form suggests the following idea about a modification of $\Gamma_{\text{MA},1}^{p-n}(Q^2)$:

$$\Gamma_{\text{MA},1}^{p-n}(Q^2) = \frac{g_A}{6} (1 - D_{\text{MA,BS}}(Q^2)) \cdot \frac{Q^2}{Q^2 + M_2^2} + \frac{\hat{\mu}_{\text{MA},4} M_4^2}{Q^2 + M_4^2} + \frac{\hat{\mu}_{\text{MA},6} M_6^4}{(Q^2 + M_6^2)^2},$$

where we added the “massive” twist-six term and introduced different masses in both higher-twist terms and into the modification factor $Q^2/(Q^2 + M_2^2)$.

The finitness of cross-section in the real photon limit leads now to

$$\Gamma_{\text{MA},1}^{p-n}(Q^2 = 0) = 0 = \frac{g_A}{6} + \hat{\mu}_{\text{MA},4} + \hat{\mu}_{\text{MA},6}$$

and, thus, we have

$$\hat{\mu}_{\text{MA},4} + \hat{\mu}_{\text{MA},6} = -\frac{g_A}{6} \approx -0.21205$$

So, we obtain

$$-\frac{g_A}{6} \cdot \frac{D_{\text{MA,BS}}(Q^2 = 0)}{M_2^2} - \frac{\hat{\mu}_{\text{MA},4}}{M_4^2} - 2\frac{\hat{\mu}_{\text{MA},6}}{M_6^2} = G,$$

where $D_{\text{MA,BS}}(Q^2 = 0) = 4/\beta_0$.

Using $f = 3$ (i.e. $\beta_0 = 9$) and putting, for simplicity, $M_2 = M_4 = M_6 = M$, we have

$$\hat{\mu}_{\text{MA},4} + 2\hat{\mu}_{\text{MA},6} = -G M^2 - \frac{2g_A}{3\beta_0} = -G M^2 - \frac{2g_A}{27} \approx -G M^2 - 0.0945$$

Taking all the results together, we have at the end:

$$\hat{\mu}_{\text{MA},6} = -GM^2 + \frac{5g_A}{54} = -GM^2 + 0.1182,$$

$$\hat{\mu}_{\text{MA},4} = -\frac{g_A}{6} - \hat{\mu}_{\text{MA},6} = GM^2 - \frac{7g_A}{27} = GM^2 - 0.3309.$$

Since the value of G is small, so $\hat{\mu}_{\text{MA},4} < 0$ and $\hat{\mu}_{\text{MA},4} \approx -0.36\hat{\mu}_{\text{MA},4} > 0$.

The fitting results of these theoretical predictions (with the condition $M_2 = M_4 = M_6 = M$), are presented in Table 4 and on Figs. 7 and 12.

	M^2 for $Q^2 \leq 5 \text{ GeV}^2$ (for $Q^2 \leq 0.6 \text{ GeV}^2$)	$\chi^2/(\text{d.o.f.})$ for $Q^2 \leq 5 \text{ GeV}^2$ (for $Q^2 \leq 0.6 \text{ GeV}^2$)
LO	$0.383 \pm 0.014 (0.576 \pm 0.046)$	0.572 (0.575)
NLO	$0.394 \pm 0.013 (0.464 \pm 0.039)$	0.586 (0.590)
N ² LO	$0.328 \pm 0.014 (0.459 \pm 0.038)$	0.617 (0.584)
N ³ LO	$0.330 \pm 0.014 (0.464 \pm 0.039)$	0.629 (0.582)
N ⁴ LO	$0.331 \pm 0.013 (0.465 \pm 0.039)$	0.625 (0.584)

Table 2: The values of the fit parameters.

As one can see in Table 4, the obtained results for M^2 are different if we take the full data set and the limited one with $Q^2 < 0.6 \text{ GeV}^2$. However, the difference is significantly less than it was in Table 3. Moreover, the results obtained in the fits using the full data set and shown in Tables 3 and 4 are quite similar, too.

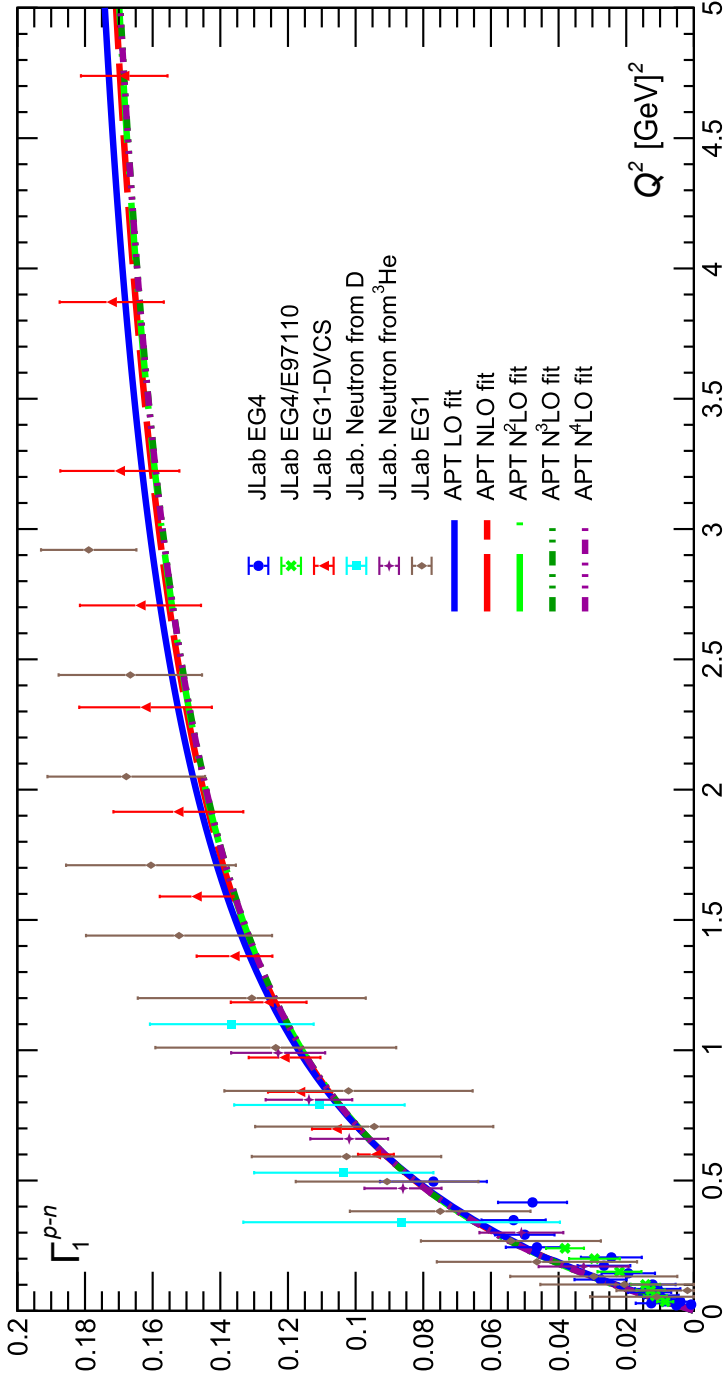


Figure 7: The results for $\Gamma_1^{p-n}(Q^2)$ in the first four orders of APT.

We also see some similarities between the results shown in Figs. 4 and 7. The difference appears only at small Q^2 values, as can be seen in Figs. 10 and 12.

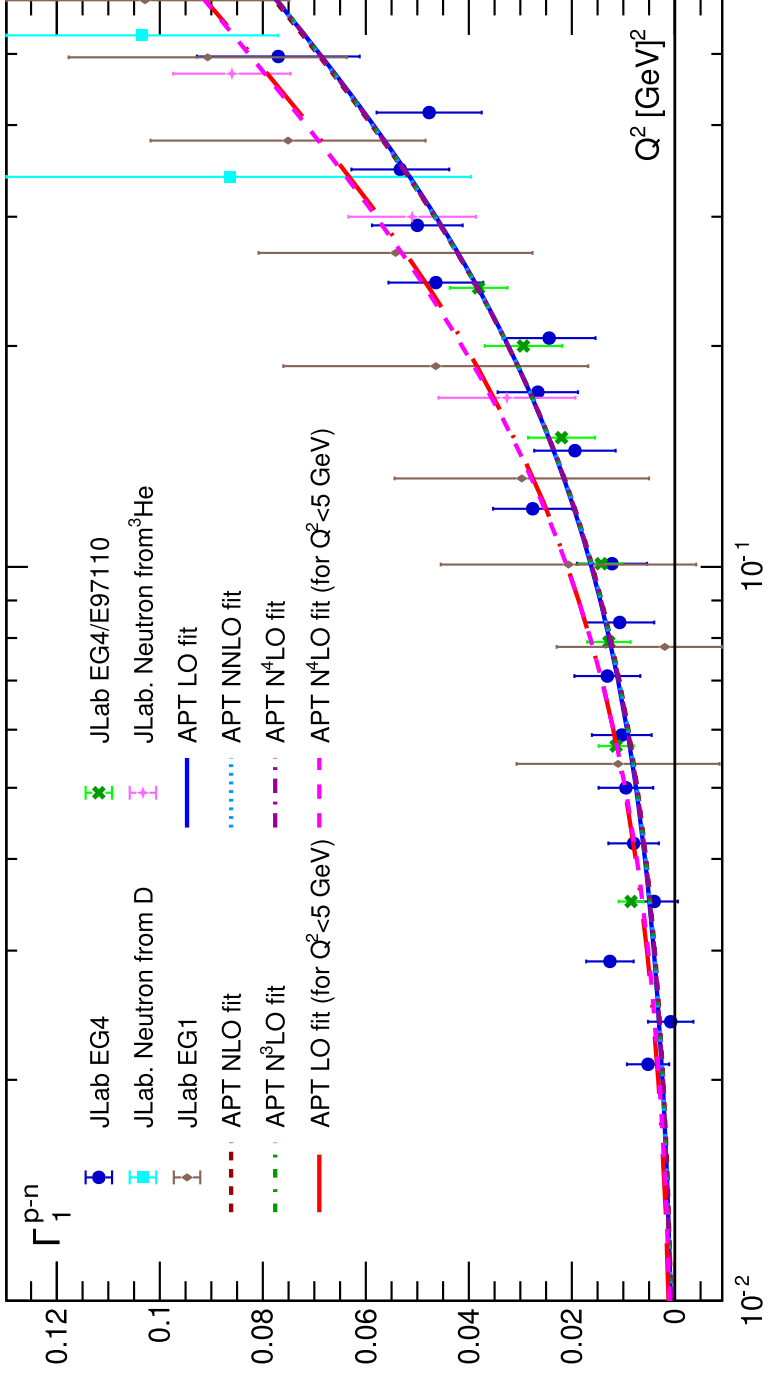


Figure 8: As in Fig. 7 but for $Q^2 < 0.6$ GeV 2

Fig. 12 also shows that the results of fitting the full set of experimental data are in better agreement with the data at $Q^2 \geq 0.55\text{GeV}^2$, as it should be, since these data are involved in the analyses of the full set of experimental data.

Of course, this low Q^2 modification is not unical. There are other possibilities. One of them can be represented as

$$\Gamma_{\text{MA},1}^{p-n}(Q^2) = \frac{g^A}{6} (1 - D_{\text{MA,BS}}(Q^2)) \cdot \frac{Q^2}{Q^2 + M_2^2} + \frac{\hat{\mu}_{\text{MA},4} M_4^2}{Q^2 + M_4^2} + \frac{\hat{\mu}_{\text{MA},6} M_6^4}{(Q^2 + M_6^2)^2}.$$

The finitness of cross-section in the real photon limit leads now to

$$\Gamma_{\text{MA},1}^{p-n}(Q^2 = 0) = 0 = \hat{\mu}_{\text{MA},4} + \hat{\mu}_{\text{MA},6}$$

and, so, we have the relation

$$\hat{\mu}_{\text{MA},4} + \hat{\mu}_{\text{MA},6} = 0, \quad \text{or} \quad \hat{\mu}_{\text{MA},4} = -\hat{\mu}_{\text{MA},6}$$

So, we have

$$\frac{g^A}{6M_2^2} \cdot (1 - D_{\text{MA,BS}}(Q^2 = 0)) - \frac{\hat{\mu}_{\text{MA},4}}{M_4^2} - 2 \frac{\hat{\mu}_{\text{MA},6}}{M_6^2} = -G.$$

Using $f = 3$ (and, thus, $\beta_0 = 9$) and also $M_2 = M_4 = M_6 = M$, we have

$$\begin{aligned}\hat{\mu}_{\text{MA},4} + 2\hat{\mu}_{\text{MA},6} &= -G M^2 + \frac{g_A}{6} \cdot \left(1 - \frac{4}{\beta_0}\right) \\ &= -G M^2 + \frac{5g_A}{54} \approx -G M^2 + 0.1182\end{aligned}$$

So, we obtain

$$\begin{aligned}\hat{\mu}_{\text{MA},6} &= -G M^2 + \frac{5g_A}{54} \approx -G M^2 + 0.1182, \\ \hat{\mu}_{\text{MA},4} &= -\hat{\mu}_{\text{MA},6} = G M^2 - \frac{5g_A}{54} \approx G M^2 - 0.1182.\end{aligned}$$

We note that at the case $M_2 = M_4$ the results of above modifications are equal and are related with the replacement:

$$\hat{\mu}_{\text{MA},4} \rightarrow \frac{g_A}{6} + \hat{\mu}_{\text{MA},4}.$$

We have verified this numerically.

4. Heavy quark contributions

Consider Heavy quark contributions. Now in MA QCD

$$\Gamma_{\text{MA},1}^{p-n}(Q^2) = \frac{g^A}{6} (1 - D_{\text{MA,BS}}(Q^2)) + \frac{\hat{\mu}_{\text{MA},4} M^2}{Q^2 + M^2},$$

where the perturbative part $D_{\text{BS,MA}}(Q^2)$ takes the form

$$\begin{aligned} D_{\text{MA,BS}}^{(1)}(Q^2) &= \frac{4}{\beta_0} A_{\text{MA}}^{(1)}, \\ D_{\text{MA,BS}}^{k \geq 2}(Q^2) &= \frac{4}{\beta_0} (A_{\text{MA}}^{(k)} + (\tilde{d}_{m-1} - \sum_{c,b,t} C_1(\xi_i)) \tilde{A}_{\text{MA},\nu=2}^{(k)} \\ &\quad + \sum_{m=3}^k \tilde{d}_{m-1} \tilde{A}_{\text{MA},\nu=m}^{(k)}). \end{aligned}$$

where

$$\xi_i = \frac{Q^2}{m_i^2} \quad \text{and} \quad m_c = 1.27 \text{ GeV}, \quad m_b = 4.18 \text{ GeV}, \quad m_c = 172.76 \text{ GeV}.$$

$C_1(\xi)$ at two-loop level: (J.Blumlein, G.Falcioni, A.De Freitas;2016)

$$C_1(\xi) = \frac{8f}{3\beta_0} \left\{ \frac{6\xi^2 + 2735\xi + 11724}{5040\xi} - \frac{3\xi^3 + 106\xi^2 + 1054\xi + 4812}{2520\xi} * L(\xi) \right. \\ \left. - \frac{5}{3\xi(\xi + 4)} * L^2(\xi) + \frac{3\xi^2 + 112\xi + 1260}{5040} * \ln(\xi) \right\},$$

$$L(\xi) = \frac{1}{2\delta} * \ln\left(\frac{1+\delta}{1-\delta}\right), \quad \delta^2 = \frac{\xi}{4+\xi}.$$

At large Q^2 values, we have

$$C_1(\xi) = \frac{2}{3\beta_0} \left\{ \frac{1}{2} - \frac{5}{12\xi^2} \ln^2(\xi) - \frac{4}{3\xi} \ln(\xi) + \frac{17}{9\xi} + O\left(\frac{\ln(\xi)}{\xi^2}\right) \right\},$$

i.e. there is the HQ decoupling here.

At low Q^2 values, it is convenient to use the approximation:

$$C_1(\xi) = \frac{2f}{3\beta_0} \left\{ 1 + \frac{4\xi}{45} + \frac{\xi^2}{420} \right\} * \ln(\xi) - \frac{58\xi}{225} - \frac{1933\xi^2}{176400} \}, \sim \ln(\xi)!!!,$$

i.e.no the HQ decoupling here.

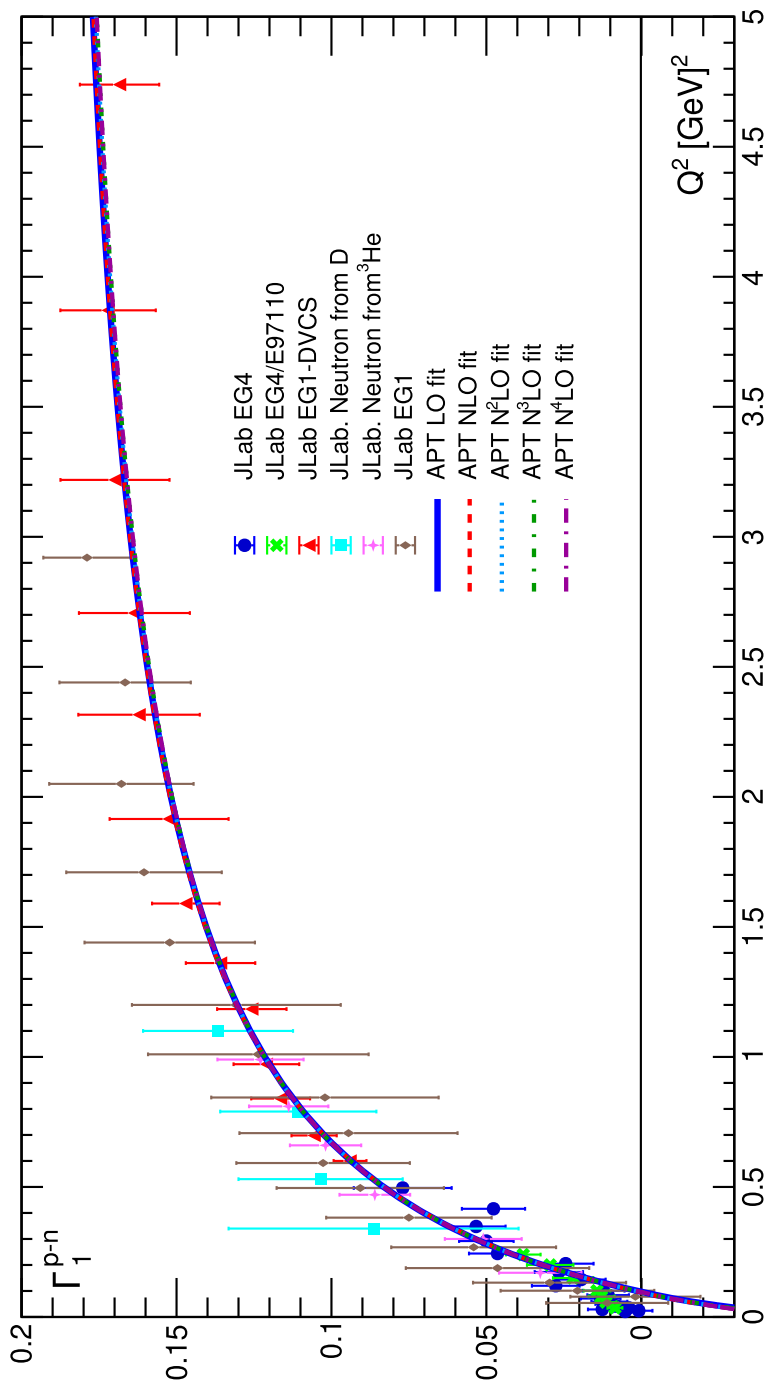


Figure 9: Same as in Fig. 4 but with heavy quark contribution.

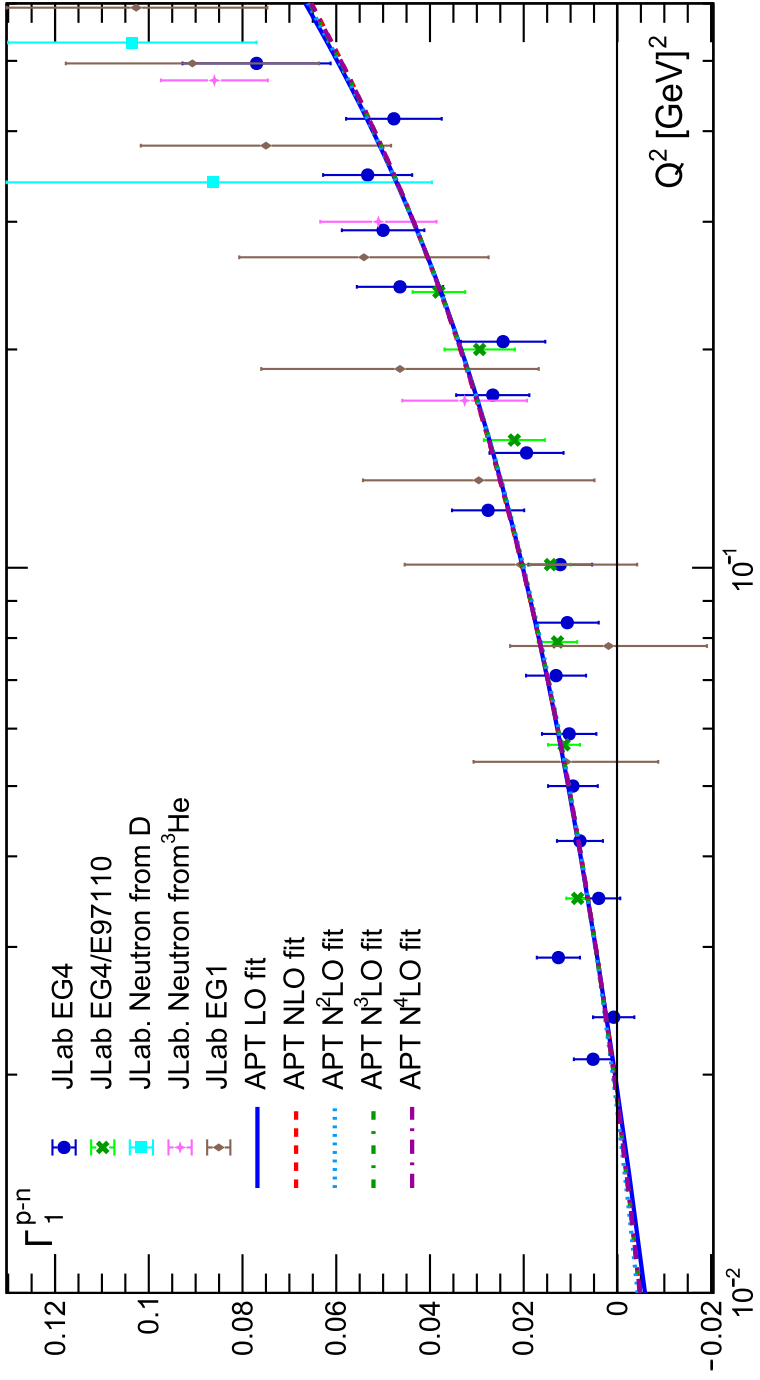


Figure 10: Same as in Fig. 6 but with heavy quark contribution.

	M^2 for $Q^2 \leq 5 \text{ GeV}^2$ (for $Q^2 \leq 0.6 \text{ GeV}^2$)	$\hat{\mu}_{\text{MA},4}$ for $Q^2 \leq 5 \text{ GeV}^2$ (for $Q^2 \leq 0.6 \text{ GeV}^2$)	$\chi^2/(\text{d.o.f.})$ for $Q^2 \leq 5 \text{ GeV}^2$ (for $Q^2 \leq 0.6 \text{ GeV}^2$)
LO	0.472 ± 0.035 (1.631 ± 0.301)	-0.212 ± 0.006 (-0.166 ± 0.001)	0.667 (0.789)
NLO	0.392 ± 0.036 (1.740 ± 0.389)	-0.196 ± 0.008 (-0.143 ± 0.002)	0.759 (0.742)
N ² LO	0.374 ± 0.036 (1.574 ± 0.319)	-0.198 ± 0.008 (-0.144 ± 0.002)	0.781 (0.714)
N ³ LO	0.372 ± 0.036 (1.588 ± 0.327)	-0.200 ± 0.009 (-0.145 ± 0.002)	0.789 (0.733)
N ⁴ LO	0.374 ± 0.036 (1.630 ± 0.344)	-0.199 ± 0.005 (-0.144 ± 0.002)	0.789 (0.739)

Table 3: The values of the fit parameters.

When we add Gerasimov-Drell-Hearn and Burkhardt-Cottingham sum rules we have

$$\Gamma_{\text{MA},1}^{p-n}(Q^2) = \frac{g_A}{6} (1 - D_{\text{MA,BS}}(Q^2)) \cdot \frac{Q^2}{Q^2 + M_2^2} + \frac{\hat{\mu}_{\text{MA},4} M_4^2}{Q^2 + M_4^2} + \frac{\hat{\mu}_{\text{MA},6} M_6^4}{(Q^2 + M_6^2)^2},$$

	M^2 for $Q^2 \leq 5 \text{ GeV}^2$ (for $Q^2 \leq 0.6 \text{ GeV}^2$)	$\chi^2/(\text{d.o.f.})$ for $Q^2 \leq 5 \text{ GeV}^2$ (for $Q^2 \leq 0.6 \text{ GeV}^2$)
LO	0.383 ± 0.014 (0.576 ± 0.046)	0.572 (0.575)
NLO	0.319 ± 0.014 (0.411 ± 0.035)	1.104 (0.630)
N ² LO	0.308 ± 0.014 (0.400 ± 0.034)	1.159 (0.621)
N ³ LO	0.309 ± 0.014 (0.411 ± 0.035)	1.181 (0.618)
N ⁴ LO	0.311 ± 0.014 (0.412 ± 0.035)	1.174 (0.621)

Table 4: The values of the fit parameters.

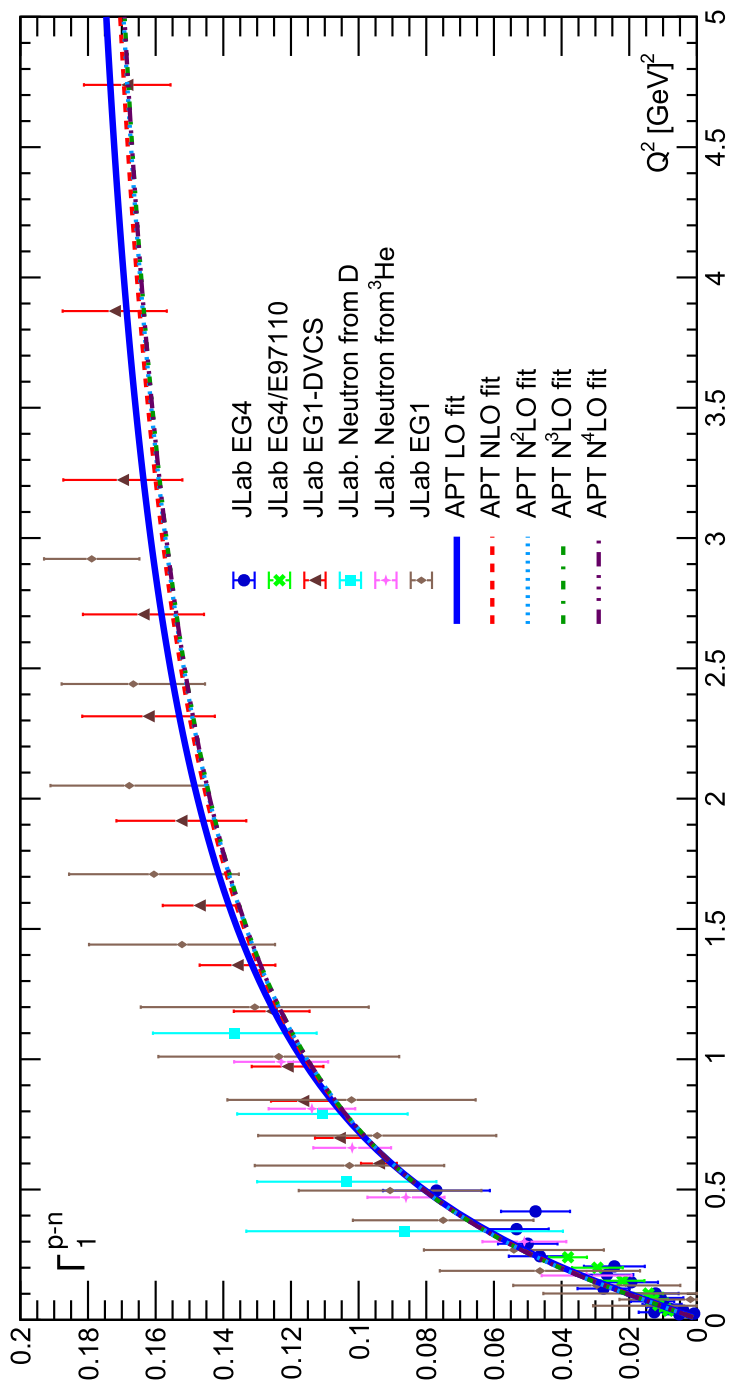


Figure 11: As in Fig. 7 but with heavy quark contribution.

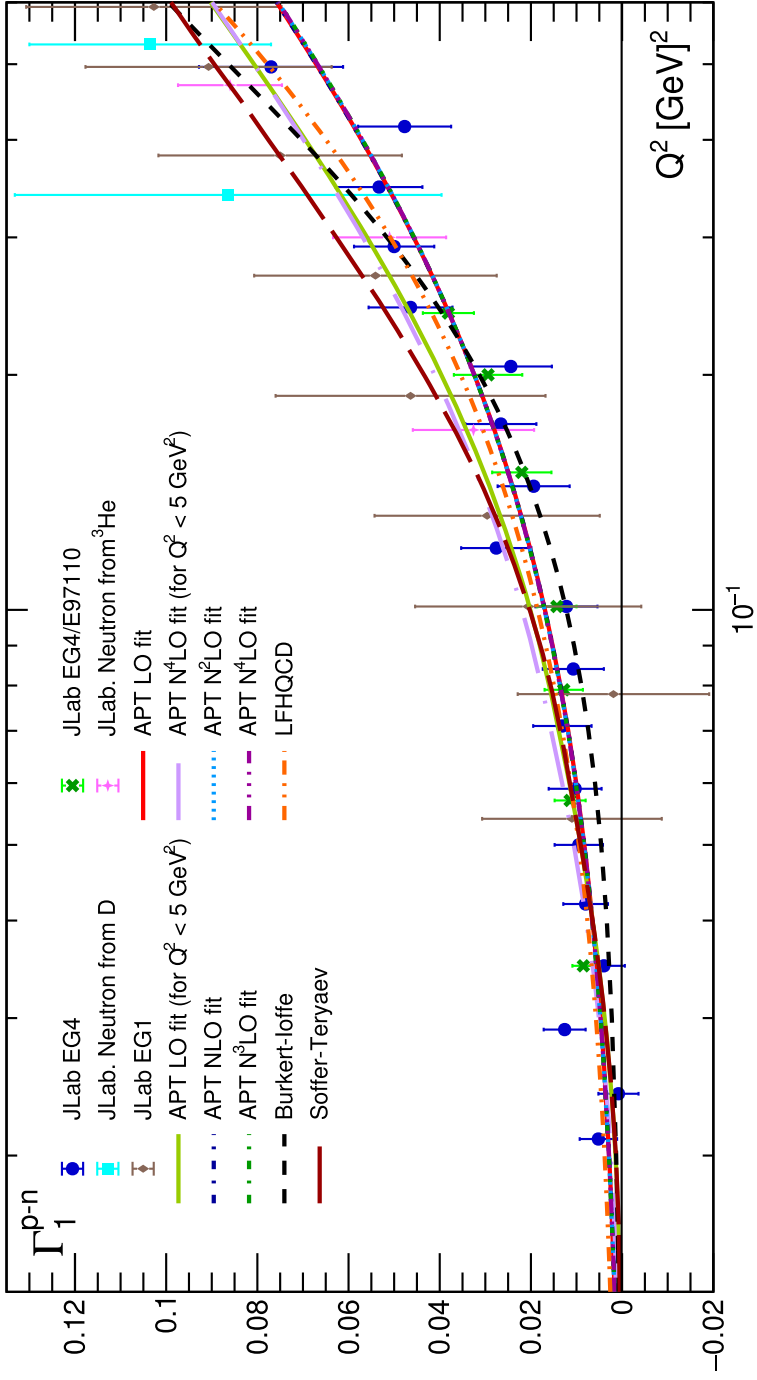


Figure 12: As in Fig. 8 but with heavy quark contribution.

5. Conclusions

We have considered the Bjorken sum rule in the framework of MA and conventional QCD and obtained results similar to those obtained in previous studies (Pasechnik et al.: 2008,2010,2012), (Ayala et al.: 2017,2018), (Kotikov, Zemlyakov: 2023) for the first 4 orders of PT.

The results based on the conventional PT do not agree with the experimental data. For some Q^2 values, the PT results become negative, since the high-order corrections are large and enter the twist-two term with a minus sign.

APT in the minimal version leads to a good agreement with experimental data when we used the “massive” version for the twist-four contributions.

Examining low Q^2 behaviour, we found that there is a disagreement between the results obtained in the fits and application of MA QCD to photoproduction.

The results of fits extended to low Q^2 lead to the negative values for Bjorken sum rule $\Gamma_{MA,1}^{p-n}(Q^2)$: $\Gamma_{MA,1}^{p-n}(Q^2 \rightarrow 0) < 0$ that contrary to the finiteness of cross-section in the real photon limit, which leads to $\Gamma_{MA,1}^{p-n}(Q^2 \rightarrow 0) = 0$. Note that fits of experimental data at low Q^2 values (we used $Q^2 < 0.6 \text{ GeV}^2$) lead to less magnitudes of negative values for $\Gamma_{MA,1}^{p-n}(Q^2)$.

To solve the problem we considered low Q^2 modifications of the perturbative part of $\Gamma_{MA,1}^{p-n}(Q^2)$.

Considering carefully one of them, we find good agreement with full sets of experimental data for Bjorken sum rule $\Gamma_{MA,1}^{p-n}(Q^2)$ and also with its $Q^2 \rightarrow 0$ limit, i.e. with photoproduction. We see also good agreement with phenomenological models.

Including the massive contribution from heavy quarks changes our results very little.